Multidisciplinary Optimization of Small Battery-Powered Aircraft for Maximum Range Flight

Kevin W. Reynolds, Ilan M. Kroo
Aeronautics/Astronautics
Stanford University
Stanford, CA, USA
kevinr2@stanford.edu, kroo@stanford.edu

Abstract - *A conceptual design approach is combined with numerical-based optimization to maximize the range of small electric aircraft of fixed battery weight. Nonlinear constraints on aircraft performance, the static and dynamic loading conditions, and a component weight breakdown are set to meet Federal Aviation Regulations and mission objectives. The optimization problem is decomposed into various discipline-specific algorithms that more broadly represent structural, propulsive, and aerodynamic models. An atmospheric model is coupled with aero-propulsion for evaluating cruise performance. Current battery technologies reveal performance limitations due to low power density. Electric propulsion efficiencies are thus driven to values greater than 70% and lift-to-drag ratios exceeding 20:1. For takeoff weights >200 lbs, range is observed to rapidly decay from that of conventional petroleum-burning aircraft of similar weight. However, potentially unmanned aircraft show an opportunity to avoid significant structural weight penalties when designed to low aspect ratios <10.*

Keywords: Multidisciplinary optimization, electric aircraft, batteries, light sport aircraft, electric propulsion.

1 Introduction

With more pressure being applied in recent years by the sudden rising price of oil and heightened awareness of global warming, fuel efficiency and emissions have appeared to the aviation industry as key drivers in the design of tomorrow's aircraft. As global passenger and cargo air travel are both projected to increase at annual rates of 4.9% and 5.4% respectively in the foreseeable future, clear indications are given that efficient aircraft and largely modified infrastructure and operations will be necessary for accommodating this increase in traffic in a sustainable way [1]. Electric power, currently supplied through the use of batteries and/or fuel cells, stands out as a likely alternative for reducing the cost of fuel and for reducing harmful emissions such as nitrous oxide and carbon dioxide. Despite challenges faced, battery technology perhaps represents the nearest term solution for improving efficiency since no 'fuel' is burned during use. Lithium polymer batteries are already being utilized by the electric vehicle (EV) automotive industry and, for this reason, were investigated further. The goal is to achieve a successful design for an extended range (>500 nmi) electric aircraft, entirely powered by batteries. With increasing government allocation of funds for the development of new electric technologies, one can be optimistic about their future applications in the design of electric airplanes. Furthermore, multidisciplinary (MDO) design tools are expected to play a significant role in electric aircraft design as a means of identifying possible configurations, analyzing system-level operation and efficiency, and improving the quality of long-term, sustainable design.

1.1 Major Challenges

Over the years, there have been a number of issues that have forestalled the widespread use and acceptance of electric aircraft. First, perhaps the most formidable of these issues or challenges has been the limitation on range due to low specific power and energy density of electric power systems. Comparatively, regular gasoline has a specific energy roughly 10 times that of the best lithium polymer battery commercially available today [2]. Second, with the hybridizing of small light sport aircraft (LSA) on average increasing an airplane's takeoff weight by 11%, fully electric aircraft design tends to increase overall weight between 11-15% [3]. This increase in weight for battery-powered aircraft often is entirely attributed to the excess weight required for carrying sufficient stored energy in the batteries. In addition, weight balance issues may become of importance to the configuration designer. Finally, inherent to the design of most battery-powered aircraft, especially, is a structural weight penalty imposed due to the constant weight of electric power systems. An issue with energy storage in batteries is the inability to burn carried fuel. The ability to burn off fuel in conventional aircraft contributes to the improvement of range as the airplane becomes lighter with time. Various types of fuel cells, including polymer electrolyte membrane (PEM) and solid oxide (SOFC), are likely candidates for use in next-generation power systems. They benefit from being able to burn their carried fuel.

Other challenges are more universal to general aviation aircraft as a whole. For small to medium-sized aircraft weighing below 50,000 lbs., stability and control issues persist for severe wind gusts and maneuver load conditions [3]. For many lightweight aircraft, including

gliders and experimental models, gust loading and maneuver are often critical and a major component in determining the operational envelope of an aircraft. Partially because of the restricted use of airspace, most general aircraft are limited to flying at relatively low altitudes below 15,000 ft. Visual flight rules (VFR) train private pilots for the operation of aircraft below this altitude [4]. Historically, flying in mountainous regions has been known to increase the likelihood of dangerous and unpredictable gust loading conditions. Flying at lower altitudes in some cases may tend to add aerodynamic drag and as a result increase fuel burn.

2 Conceptual Design

Certain expectations existed going into the optimization process based on previous design examples and conceptual knowledge. For maximizing range or reducing drag at cruise, it was expected that possible configurations would be designed to have high lift-to-drag ratios (*L/Ds*), comparable to those achievable by glider-like aircraft such as the Pipistrel Taurus [5]. Both tractor and pusher configurations were considered for all design cases. From a conceptual point of view, it seemed preferable to use pusher prop configurations whenever possible for reducing swirl over the fuselage and wing and for reducing pressure drag. Due to the increase in weight, manned aircraft generally demand a higher lift coefficient C_L at takeoff than unmanned aircraft, a requirement that tends to encourage the use of the tractor configuration to better accommodate a larger propeller(s).

2.1 Aerodynamic Design

It was expected that a high aspect ratio wing of fixed surface area, and thus high span, would be necessary for improving aerodynamic cleanliness, achieving high C_L, and maintaining a relatively low Reynolds number on the wing at cruise. The following equation for span was used:

$$b = \sqrt{\frac{mgAR}{W_{to}/S_{ref}}} = \sqrt{mgAR/\Sigma} \qquad (1)$$

where mg and W_{to} are the maximum takeoff weight, AR is the wing aspect ratio, S_{ref} is the wing reference area, and Σ is the takeoff wing loading. The wing loading was an important quantity also to the determination of the stalling speed [6].

For the purpose of reducing skin friction drag at cruise, small wing area would be preferred to larger area. Additionally, the small chords would allow for low Reynolds numbers across the wing and be more conducive to extensive runs of natural laminar flow [3]. This would potentially offer additional zero lift drag savings at cruise. For reducing lift drag at takeoff and landing a high span wing would be preferred. Assuming a parabolic drag polar, the equation for best *L/D*:

$$\left.\frac{L}{D}\right|_{best} = \frac{1}{2}\sqrt{\frac{\pi AR}{C_{Do}}} \qquad (2)$$

was used for understanding the relationship between the wing aspect ratio and the zero lift drag coefficient C_{Do} affected by Reynolds number. Because of the initial expectation of a high aspect ratio wing at fixed wing area for high span, most wing configurations were assumed to be high-mounted on the fuselage. When subject to certain span constraints, wing tip extensions, winglets, and C-wing configurations might provide real alternatives for increasing the effective aspect ratio and span of the wing for minimizing lift-dependent drag.

2.2 Propulsion Design

The propulsion energy source for this study of aircraft design was lithium polymer batteries. The choice was made based on the relatively low total weight required for integration, the high operation efficiencies >90%, and the reliability shown through applications in the automotive industry [2, 5]. Other prime candidates included PEM and SOFCs. Neither was chosen due to the relatively low operation efficiencies (<60%) and total system weight [7]. The total system weight of the fuel cells would include fuel processing, air pressurization, and waste elimination.

To ameliorate stability and control issues, the batteries were located directly behind the pilot. This concentrated the total weight distribution closer to the airplane's center of gravity in order to minimize necessary tail and control surface sizes. This configuration layout for the batteries was also used on the Pipistrel Taurus Electro [5].

The propeller location would depend on the electric motor sizing, the possible need for a gearbox, and ground clearance constraints at takeoff and landing.

3 Problem Formulation

The feasible design space was analyzed by decomposing the problem into an objective function, design disciplines, constraints, and a performance model

3.1 Objective Function Selection

A number of potential objective functions were considered for the optimization problem. With the most sizable challenge in electric aircraft design being a sustained duration of flight greater than an hour, it would perhaps be useful to maximize any of the aerodynamic, propulsive or structural factors contributing to range [6]. The wing design perhaps would be more important to overall performance in cases where propulsive power was limited.

Subsequently, *L/D* was considered as a possible objective function. Having certain restrictions placed on flight altitude by VFR for general aviation pilots made maximizing this function a more difficult problem to approach. Often the best *L/D* is achieved at higher altitudes. In addition, this function would only serve to measure aerodynamic efficiency, thus neglecting the impact of propulsion and structures on the overall performance.

In most aircraft design problems, the weight of the aircraft can also be used as a figure of merit for determining cost. Minimizing such an objective function might be useful to the design of low-cost, ultra-light or experimental aircraft. Over the years, relationships have been established between the takeoff weight of an aircraft and the cost of manufacture. For large commercial airliners, $500 per pound gives a reasonable approximation of cost [6]. For smaller airplanes, a relationship between cost and weight more strongly depends on the type of aircraft and its mission requirements. For electric aircraft, the use of batteries or fuel cells disproportionately impacts this cost/weight relation. For this study of a battery-powered aircraft, battery weight was agreed upon initially as the best objective function for minimizing both cost and weight while maximizing performance.

A first attempt to arrive at an optimal configuration by enforcing nonlinear constraints on performance used the objective function of battery weight. The battery weight was calculated by subtracting component weights from the maximum takeoff weight W_{to}. As posed, the minimization of battery weight was dependent on the takeoff weight used as a design variable for determining various component weights via known empirical relations. The takeoff weight was forced to minimal values along with the battery weight, hurting both cruise performance and range in the process.

A new objective function was later chosen. Being a more appropriate measure of performance, range was ultimately chosen as the objective function represented as a product of the cruise velocity and runtime of the engine. Expressing range as a function of the total energy available from a battery yielded the following:

$$R = \frac{\eta_{ov} V_{cr} E_{avail}}{P_{req}} \tag{3}$$

where η_{ov} is the overall system efficiency, V_{cr} is the cruise velocity, E_{avail} is the energy available as a function of the battery weight, and P_{req} is the power required to overcome drag at cruise. The overall efficiency is defined as the product of the propeller efficiency (defined later in Section 4.3) and the motor and gearbox efficiencies given in Table 1.

A distance equivalent to 30 minutes flying at the given cruise condition was subtracted from the range to account for necessary reserve energy [4, 5]. Using this objective function required that constraints be placed on aircraft performance and on component weights. The minimum allowable range used was 200 nmi. This setup allowed a much smoother function evaluation. The parameters and constants are listed below:

Table 1. Assumed values for parameters and constants.

Parameters and Constants	Value
Wing thickness ratio *t/c*	0.15
Tail thickness ratio	0.1
Wing taper ratio *λ*	1
Horizontal tail aspect ratio	5
Vertical tail aspect ratio	2.5
Wing sweep *Λ*, [degrees]	0
Maneuver load factor *nmax*	3.8
Semi-span wing panels *np*	30
Inviscid Oswald efficiency *uinviscid*	1
Interference factor	0.975
Gravitational acceleration, [ft/s²]	32.2
Air density @ SL, [slug/ft³]	0.00237
Maximum wingbox stress, [psi]	54,000
Motor efficiency *ηmotor*	0.95
Gearbox efficiency *ηgearbox*	0.9
Structural wingbox density *ρs*, [slug/ft³]	5.4
Nonstructural wingbox weight *w0*, [lb]	1

3.2 Design Variable Selection

Design variables were selected that appropriately described the simplified geometry and configuration layout of the design. It was desirable to choose the fewest number of variables necessary for capturing meaningful variation in the design for the lowest computational cost. As an initial metric of payload capability, the takeoff weight was selected as a variable for determining the usability of the design, either as a manned or unmanned aerial vehicle. The wing area was chosen for its importance to aerodynamic performance and for its common recurrence throughout the performance relations [8]. The aspect ratio represented a second degree of freedom in the design of the wing planform and was also favored as a non-dimensional quantity. The power of the engine was included as a variable necessary for estimating the engine weight based on empirical data [8]. The variation in propeller diameter was incorporated into the design of the propulsion system for its effect on system efficiency. The cruise velocity was used for its influence on the range while altitude served to describe the atmospheric conditions for the generation of thrust and lift at cruise. The seven design variables chosen are listed in Table 2.

Table 2. List of design variables and the assumed minimum and maximum values.

Variable	Description	Minimum	Maximum
Peng, [kW]	Max engine power	5	40
AR	Wing aspect ratio	5	30
Sref, [ft²]	Wing reference area	5	200
hcr, [ft]	Average cruise altitude	100	15,000
Vcr, [kts]	Average cruise velocity	50	200
Wto, [lbs]	Max takeoff weight	50	1,300
dprop, [in]	Propeller diameter	10	100

4 Decomposition Modeling

The optimization problem was decomposed into the following models in order to better isolate the importance of each discipline to the overall design.

4.1 Atmospheric Model

A model of the 1974 Standard Atmosphere was included in the optimization [3]. With all operation expected to occur inside the troposphere, the dynamic pressure was assumed constant at the design cruise altitude. The variations in pressure, density, temperature, viscosity, and speed of sound affected directly the values calculated for the non-dimensional quantities of Reynolds number and Mach number. With operation speeds below M<0.3, the effect of compressibility on C_{Lmax} was considered negligible.

4.2 Aerodynamic Model

The purpose of the aerodynamic model was to identify the lift and drag characteristics of the wing, tail, and fuselage. An elliptical lift distribution was assumed over a rectangular, unswept wing for minimum induced drag. This implied a twist distribution across the wing and a constant downwash. The corresponding maneuver lift coefficient distribution changed by a constant amount with angle of attack and total lift by the following relation:

$$C_{lm}(y) = C_{lcr}(y) + C_{Lm} - C_{Lcr} \tag{4}$$

where y is the spanwise coordinate. Thus, the local lift coefficient distribution C_{lcr} at cruise was determined by dividing the wing semi-span into 30 uniformly distributed spanwise sections n_p. The C_{Lcr} was set by takeoff weight, dynamic pressure, and wing area. The maneuver lift coefficient C_{Lm} was determined as the product of the limit load factor 3.8 for general aviation and $C_{Lcr.}$

The C_{Lmax} was calculated at both takeoff and landing from a reference Reynolds number and C_{Lmax} of $5\text{x}10^6$ and 1.35 respectively [9]. C_{Lmax} was used for determining the stalling speeds.

A total drag coefficient of the airplane was written as the sum of the zero lift and lift dependent drag coefficients, C_{Do} *and* C_{Di} respectively, as:

$$C_D = C_{D0} + C_{Di,viscous} \tag{5}$$

and used a component breakdown of the wing, fuselage, and tail by form factor and Reynolds number to determine the individual contributions to zero lift drag. The lift-dependent drag coefficient was determined under the elliptical lift assumption from the total lift coefficient C_L. The viscous Oswald span efficiency was determined from the following relation:

$$u_{viscous} = \frac{1}{\pi AR \cdot K \cdot C_{D0} + 1/u_{inviscid}} \tag{6}$$

The factor K was determined from empirical data and the value for the inviscid Oswald efficiency $u_{inviscid}$ is provided in Table 1. An interference factor between wing and fuselage of 0.975 was assumed [3].

4.3 Propulsion Model

A propeller-driven propulsion system was modeled for its expected high efficiency at cruise at low Mach numbers. A sizing model for the engine assumed 1 horsepower per pound of engine. This ratio matched the 2007 industry standard (See Ref. [5]). Based on emphirical data collected from the Pipistrel Taurus and Electroflyer, the rotational speed of the propeller was assumed relatively low at 1800 rev/min. The advance ratio was calculated as the ratio of the forward to tangential velocities. This advance ratio was used to determine the thrust coefficient at the cruise condition and the efficiency of a lightly-loaded, inviscid disc propeller from the following equations:

$$C_T = \frac{T}{\rho n^3 d_{prop}^{\ 5}} \tag{7}$$

$$\eta_{prop} = \frac{1}{1 + 2T/\rho\pi(d_{prop}V_{cr})^2} \tag{8}$$

where T is the thrust/drag at cruise, ρ is the air density, n is the number of rotations per second, d_{prop} is the propeller diameter, and V_{cr} is the cruise velocity.

4.4 Structures Model

The total takeoff weight was handled as a sum of individual component weights. The maximum takeoff weight was free to change as a design variable and a predefined battery weight was used for each run. The wing weight W_{wing} was calculated as the sum of wing section weights w_i along the span according to the following equations:

$$w_i = c_i(2gy_i\rho_s t_{s,i}c_{box} + w_0) \tag{9}$$

$$W_{wing} = 2\sum_{i=1}^{np} w_i dy \tag{10}$$

where i is the spanwise index of the wing section, ρ_s is the structural density of the wingbox, $t_{s,i}$ is the skin thickness distribution, c_{box} is the constant wingbox chord ratio, c_i is the chord distribution, w_0 is the weight of the non-structural part of the wing section, and n_p is the number of sections along the semi-span [3]. The total wing weight was due to both the weight and inertia of the wing.

It was assumed that wing spars took pure bending loads and the wing skins took flexural shear. With typical wing skin thicknesses allowed to vary anywhere from 1 inch at the wing root to a minimum gauge of 0.06 inches at the wing tip [3], an initial skin thickness distribution along the spanwise direction was first assumed and incremented in order to achieve a relatively constant shear stress across the wing independent of wing loading Σ.

An iterative algorithm was used for incrementing the initial skin thickness distribution by comparing the shear stress at the wing root and tip determined by the local bending moment at each section of the wing. The moment was calculated using simple beam theory under the assumption of small bending deflections, local perpendicular cross sections, and elastic materials. A thickness increment of 1/700 of an inch was applied at the end of the wing having the higher stress until the two values converged within a tolerance of 100 psi. This method represented a simple approach for approximating a uniform shear stress distribution across the wing at the static condition.

5 Design Constraints

In order to guarantee each design's compatibility with VFR and LSA rules and the satisfaction of basic design requirements, nonlinear constraints were used to place upper or lower bounds on relevant performance quantities.

5.1 Stalling Speed

The constraint placed on the stall speed at takeoff was decided upon in order to meet the stall speed requirements established by the Federal Aviation Administration (FAA) for LSA. LSA are required to have a maximum stall speed of 45 knots and a maximum cruise speed of 120 knots (See Ref. [4]). The general equation for stall speed was used under the assumption that lift was equal to weight during takeoff and landing. A takeoff speed of 1.2 times V_{stall} and a flap deflection angle of 20° was assumed. Flaps were not fully deflected at takeoff for low drag. Landing speed was taken to be 1.3 times V_{stall} at a flap deflection angle of 40° like the SWIFT glider. No leading edge devices were assumed.

5.2 Takeoff and Landing Field Lengths

Due to the VFR certification training required for private pilots, the majority of small aircraft under 12,500 pounds were expected to fly out of private/general aviation airports with average runway lengths less than 7,000 feet. For what was to become a LSA, these field lengths were limited more aggressively to 1,500 feet. The takeoff field length was calculated assuming that one engine operation was not critical for the length determination of the runway. With little information known about the dynamics of the landing gear and/or the traction of the runway, the following equation for military or small civil aircraft was used for calculating the Federal Aviation Regulation (FAR) Part 23 takeoff field length, or the distance required to clear a 50 foot obstacle shortly after lift-off:

$$TOFL_{prop} = 5.75 \cdot P_{eng,inst}\left(\frac{\sigma N d_{prop}^{\,2}}{P_{eng,inst}}\right)^{1/3} \qquad (11)$$

where $P_{eng,inst}$ is the maximum installed shaft engine power at takeoff, σ is the takeoff air density ratio to sea level, and N is the number of engines [8].

5.3 Climb Rate and Operation Ceiling

The horizontal component of climb speed V_{cl} was taken to be 1.3 $V_{stall,to}$ in the second segment of climb. By FAR Part 25 standards, the minimum climb gradient for a single-engine airplane was 2.4° [3, 8]. The climb rate was calculated from the following equation:

$$\dot{h} \approx V_{cl}\sin\gamma = V_{cl}\left(\frac{T-D}{W_{to}}\right) \qquad (12)$$

with the gradient/angle of climb γ, the thrust T and drag D calculated at 400 feet, and the takeoff weight W_{to}.

Operational ceiling defined for general aircraft is the altitude at which the climb rate given in Equation (12) is equal to 500 ft/min. Thus, the maximum operational ceiling was limited to 15,000 feet by FAR Part 91 stating that no person operating a “civil aircraft of U.S. registry be unsupported at this altitude by supplemental oxygen." [8] For this study, the same maximum operational altitude was applied to unmanned aircraft configurations.

6 Aircraft Design Results

A gradient-based optimizer was used evaluating the following problem:

maximize	Range
with respect to	$\{P_{eng}, AR, S_{ref}, h_{cr}, V_{cr}, W_{to}, d_{prop}\}$
subject to	Stalling speed @ sea level < 45 kts
	Takeoff field length < 1,500 ft
	Landing field length < 1,500 ft
	Second segment Climb @ 400 ft > 2.4°
	Operational ceiling < 15,000 ft
	W_{to} – Component Weights > 0

More than 60 unevenly distributed grid points were used to create a surface plot of the maximum cruise range achievable as a function of non-dimensional quantities (See Figure 1a).

Given a fixed fuel/battery weight, the optimizer determined the best takeoff weight for each configuration. This ratio was referred to as the fuel weight fraction W_f / W_{to}. The small electric aircraft configurations generated were separated into two main categories based on their fuel weight fraction: manned and unmanned. The criteria used for identifying possible manned aircraft was based on a minimum pilot weight allowance of 100 lb pilot and 50 lbs of empty weight. These numbers were assumed based on a comparison with other low-powered aircraft such as Aerovironment's Gossamer, the Solar Challenger, and SWIFT glider. Consequently, the lightest of the manned configurations was characterized by fuel volume limitations that compromised the ability to carry a passenger. The boundary shown in Figure 1b separating manned from unmanned aircraft roughly coincided with the region dividing fuel limitations from increasing drag due to high Reynolds number. At high wing aspect ratios, the boundary tended to higher fuel weight fractions for achieving maximum range. In Figure 2, the minimum battery weight for an aircraft of given takeoff weight and wing aspect ratio 20 was shown to be approximately 100 lbs.

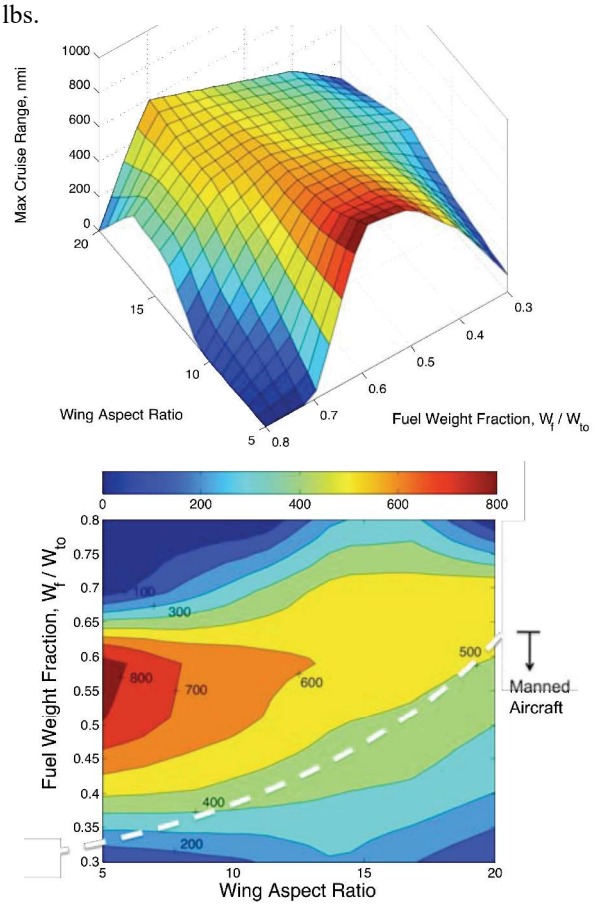

Figure 1. (a) Surface plot and (b) contour map of cruise range as a function of two non-dimensional quantities, wing aspect ratio and fuel weight fraction. 'Manned aircraft' demarcation line is based on 150 lbs. minimum empty weight requirement.

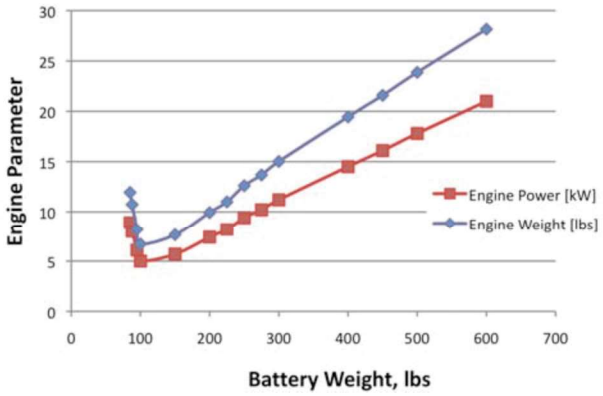

Figure 2. Optimal battery weight as a function of engine power and weight for a wing aspect ratio of 20.

7 Conclusions and Future Work

Using battery power as an energy source for electric propulsion adds a rather dramatic structural weight penalty that can be associated with the dilemma of having to "consume/burn fuel to carry fuel" over the entire mission. Conventional aircraft are able to gain a performance advantage as fuel is burned and the aircraft becomes lighter. This bonus allows the aircraft to climb to higher altitudes in the latter end of the cruise segment where thrust is increased relative to drag and the engines can be further throttled back to save fuel. At higher takeoff weights, the penalty for carrying electric power systems tends to increase dramatically, encouraging the use of more conventional fuels with higher energy density. At these higher takeoff weights, the square-cube law predicts more structurally inefficient designs that limit range when propulsive energy is in short supply. The square-cube law states that the surface area of an object grows as the square of the size while the weight/volume of an object grows as size cubed.

The weight required to build an aircraft, roughly empty weight, becomes more dominant with respect to impact on range when propulsive energy provided by the batteries is limited. The heavier the fuel tank (or the amount of energy carried), the more benefit can be gained from burning it off over the life of the mission. The results in Figure 1b show that for low aspect ratio electric aircraft, it is possible to get more range for less fuel carried. However, the takeoff weight also tended to decrease with wing aspect ratio leaving less available weight for a person and making the aircraft generally unmanned. Resolving a lower bound on aspect ratio for improved range in electric unmanned aerial vehicles and improving the fidelity of the propulsion model will be the topics of further research.

Acknowledgments

We gratefully acknowledge financial support from the National Science Foundation, Boeing, and NASA.

References

[1] National Aeronautics and Space Administration, "NASA and the next generation air transportation system (NEXTGEN)," 2007, http://www.aeronautics.nasa.gov/docs/nextgen_whitepaper_06_26_07.pdf.

[2] M. Moore, "Electric propulsion enabled advanced air vehicles," 2008 CAFE Foundation Electric Aircraft Symposium, San Francisco, April 2008.

[3] I. Kroo, *AA241 Notes: Aircraft design: Synthesis and analysis*. http://adg.stanford.edu/aa241/, (Updated 2009).

[4] Experimental Aircraft Association, "Sport pilot," http://www.sportpilot.org/index.html (Updated 2009).

[5] I. Boscarol and T. Tomazic, "Taurus Electro – The future now," 2008 CAFE Foundation Electric Aircraft Symposium, San Francisco, April 2008.

[6] M. Drela, J.M. Protz and A.H. Epstein, "The role of size in the future of aeronautics," AIAA International Air and Space Symposium and Exposition: The Next 100 Years, Dayton, OH, Paper no. AIAA-2003-2902, July 2003.

[7] German Aerospace Center (DLR), "DLR motor glider Antares takes off in Hamburg – Powered by a fuel cell," July 2009, http://www.dlr.de/en/desktopdefault.aspx/tabid-1/86_read-18278/.

[8] J. Roskam, *Airplane design: Part VII Determination of stability, control, and performance characteristics: FAR and military requirements*, DARcorporation, Lawrence, KS, 1988.

[9] D. Raymer, *Aircraft design: A conceptual design approach*, AIAA Education Series, AIAA Inc., Reston, VA, 2006.